PROCEEDINGS OF SPIE

SPIEDigitalLibrary.org/conference-proceedings-of-spie

Optical system visualization of combined reflectance model based on cubic and quadratic functions

Oleksandr Romanyuk, Yevhen Zavalniuk, Nataliia Titova, Oleksandr Kaduk, Waldemar Wójcik, et al.

Oleksandr Romanyuk, Yevhen Zavalniuk, Nataliia V. Titova, Oleksandr Kaduk, Waldemar Wójcik, Maksat Kalimoldayev, Zhazira Shermantayeva, "Optical system visualization of combined reflectance model based on cubic and quadratic functions," Proc. SPIE 12985, Optical Fibers and Their Applications 2023, 129850C (20 December 2023); doi: 10.1117/12.3023138

SPIE.

Event: Optical Fibers and Their Applications 2023, 2023, Lublin, Poland

Optical system visualization of combined reflectance model based on cubic and quadratic functions

Oleksandr Romanyuk[a*], Yevhen Zavalniuk[a], Nataliia V. Titova[b], Oleksandr Kaduk[a], Waldemar Wójcik[c], Maksat Kalimoldayev[d], Zhazira Shermantayeva[e]
[a]Vinnytsia National Technical University, Vinnytsia, Ukraine; [b]National University "Odessa Polytechnic", Odessa Ukraine; [c]Lublin University of Technology, Lublin, Poland; [d]Institute of Information and Computational Technologies CS MES RK, Almaty, Kazakhstan; [e]Al-Farabi Kazakh National University, Almaty, Kazakhstan

ABSTRACT

In the article the combined reflectance model based on quadratic and cubic polynomials is discussed. The main characteristics of physically accurate Torrance-Sparrow, Löw models and empirical Blinn, Phong, Schlick models are analyzed. The advantages and disadvantages of the cubic and quadratic Blinn-Phong model approximations are explored. The need in the development of new Blinn-Phong model approximation through combining the quadratic and cubic functions is justified. The cubic model is improved in order to improve the accuracy of Blinn-Phong model approximation in the attenuation zone. The formulas of the improved cubic model coefficients are simplified. The precise and approximated formulas for the calculation of connection point between quadratic and cubic functions are obtained. The productivity gain from the replacing the cubic function by the quadratic function in the glare's epicenter zone is calculated. The absolute and relative errors of Blinn-Phong model approximation by the quadratic, cubic and the proposed model are compared. Through the visualization of the test figures "Teapot" and "Robot" the advantages of the proposed function usage for increasing the realism of glares formation are shown.

Keywords: optical system, reflectance model, cubic model, quadratic function, polynomial function, rendering

1. INTRODUCTION

During the formation of the three-dimensional graphics images the highly accurate reproduction of the scene objects' features is important. Among the approaches to highly realistic rendering are the increasing of surface polygons numbers, ray tracing, realistic textures mapping, anti-aliasing, the usage of the complex models of light reflectance from the surfaces. The providing of high realism of the image increases the full time of its forming, it does not always complies with the requirements of modern graphics systems. The objects' surfaces shading procedure1 is the most computationally expensive substage of rendering. At this substage the color intensity is obtained for every point of the image. The productivity of color intensity calculation strongly depends on the complexity of the used light reflectance model.

The existing models of light reflectance from surface don't always comply with the high realism and high productivity characteristics[1]. Therefore, the development of light reflectance models, that increase the accuracy of representing the light reflection from the objects' surfaces and increase the productivity of surfaces shading, is actual.

2. THE LITERATURE OVERVIEW

For representing the optical characteristics of material relative to the illumination source and camera positions changes the bidirectional reflectance distribution function (BRDF)[2] is used. BRDF is calculated using the formula[3].

$$BRDF = \frac{dI(\vec{V_i})}{I(\vec{L_i})\cos\alpha_i d\omega_i}$$

where $d\omega$ - differential solid angle, $I(\vec{V_i})$ - the light intensity in the direction to the viewer, $I(\vec{L_i})$ - the light intensity

*e-mail: rom8591@gmail.com

Optical Fibers and Their Applications 2023, edited by Waldemar Wójcik, Zbigniew Omiotek, Andrzej Smolarz, Proc. of SPIE Vol. 12985, 129850C · © 2023 SPIE
0277-786X · doi: 10.1117/12.3023138

in the direction to the light source.

Torrance-Sparrow [4,5] and Löw[6] BRDFs are classified as physically accurate reflectance models. The disadvantage of physically accurate models is a high computational complexity. Torrance-Sparrow BRDF [4,5] lies in taking into account the surface roughness through using the micro-facets regions. The model involves the calculation of Gauss or Beckmann micro-facet distribution, the Schlick approximation of the Fresnel factor, Geometric attenuation factor. The model is calculated using the formula [7]

$$\frac{DFG}{4\pi(\vec{L}\vec{N})},$$

where D -micro-facet distribution, F - Fresnel factor, G - Geometric attenuation factor, $\vec{L}$ - vector to the source of light, $\vec{N}$ - normal to the surface.

Micro-facet Löw BRDF[6] is the improvement of Cook-Torrance model and lies in using the ABC-like micro-facet distribution. The specular component of model is calculated using the formula

$$\frac{S(\sqrt{1-(\vec{H}\vec{N})})FG}{(\vec{L}\vec{N})(\vec{N}\vec{V})},$$

where $\vec{V}$ - vector to the viewer, $\vec{H}$ - half-vector between $\vec{V}$ and $\vec{L}$, S - the ABC-like distribution function.

The empirical light reflectance models, among which are Phong[8], Blinn[9] and Schlick[10] BRDFs, are highly productive but they less accurately reproduce of the optical characteristics of surfaces.

Phong BRDF[8] involves the angle ψ calculation between $\vec{V}$ and specular reflectance vector $\vec{R}$. Blinn BRDF[9] lies in the improvement of Phong BRDF through the replacing the ψ angle by the γ angle between $\vec{N}$ and $\vec{H}$. Blinn-Phong model is calculated using the formula

$$\cos(x)^n,$$

where x - the angle (ψ or γ), n - the surface shininess coefficient, it corresponds to the diapason $[1,1000]$.

When the values of n are big the Blinn-Phong BRDF doesn't comply with requirement of highly productive image formation. Therefore the Blinn-Phong BRDF approximations are used. Among the approximations are Schlick function, the polynomial cubic and polynomial quadratic functions.

The Schlick function[10,11,12] is characterized with the elimination of the exponential computational complexity increasing during the increasing of n. The disadvantage of function is not accurate enough reproduction of the attenuation zone. The function is calculated using the formula[13,14]

$$\frac{\cos(\gamma)}{n-n\cos(\gamma)+\cos(\gamma)}.$$

The quadratic polynomial function[11,15], which is used for Blinn-Phong model approximation, is calculated using the approximate formula[11,16]

$$0.786n\cdot\cos(\gamma)^2+(1-0.786n)\cdot\cos(\gamma).$$

The quadratic function reproduces the glare in the epicenter zone quite accurately but leads to unnatural attenuation zone representation, because this function is a parabola and falls too fastly to the level of the ordinate axis zero. The another disadvantage of function is the need in the clipping operation performing because of the ordinate axis crossing.

The cubic polynomial function[11] for Blinn-Phong model approximation is calculated using the formula

$$A\cos(\gamma)^3+B\cos(\gamma)^2+C\cos(\gamma)$$

where A,B,C - coefficients.

The coefficient A is calculated using the formula

$$\frac{LR(R-L)+GR(1-R)+LQ(L-1)}{L^3(R-R^2)+L^2(R^3-R)-LR^2(R-1)},$$

where Q - the ordinate axis point at the level $\cos(t)^n$, G - the ordinate axis point at the level $\cos(u)^n$ (is located near ordinate axis zero), t,u - the abscissa axis points, $R=\cos(t)$, $L=\cos(u)$.

The coefficient B is calculated using the formula

$$\frac{GR(R^2-1)+LR(L^2-R^2)+QL(1-L^2)}{L^3(R-R^2)+L^2(R^3-R)-LR^2(R-1)}.$$

The coefficient C is calculated using the formula

$$\frac{GR(R-R^2)+L^2Q(L-1)+LR(LR^2-L^2R)}{L^3(R-R^2)+L^2(R^3-R)-LR^2(R-1)}.$$

As the Q, G it's recommended to use the values $0.5, 1/18$ [11] respectively.

Let's denote the Blinn-Phong BRDF as F_B, its quadratic approximation as F_{KV}, its cubic approximation as F_{KUB}. Fig. 1 shows the plots of F_B, F_{KV}, F_{KUB} .when $n=80$.

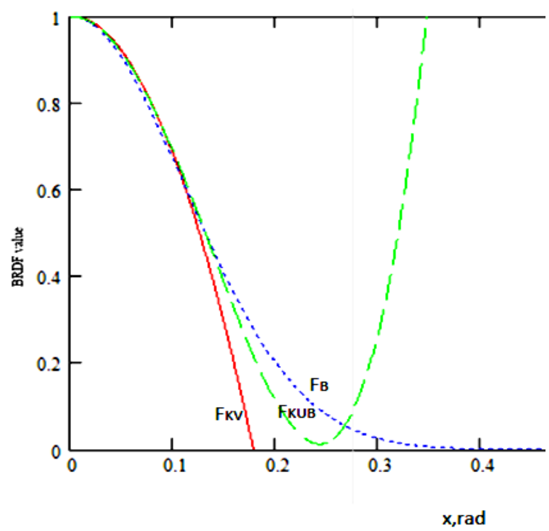

Figure 1. The plots of F_B, F_{KV}, F_{KUB} .when $n=80$

As shown in the picture, the plot of F_{KV} in the glare's epicenter zone approximately coincides with the F_{KUB} plot. Therefore, in the epicenter zone it's advisable to calculate F_{KUB} as F_{KV}. The another direction of F_{KUB} improvement is increasing the approximation accuracy of the glare's attenuation zone.

The aim of the work is development of combined surface reflectance model that provides the increasing of cubic model calculation productivity and increasing of the accuracy of attenuation zone reproduction.

3. THE DEVELOPMENT OF COMBINED BRDF BASED ON CUBIC AND QUADRATIC FUNCTION

The proposed BRDF includes the F_{KV} calculation in the glare's epicenter zone and the improved F_{KUB} calculation in the attenuation zone.

Let us find the modified cubic function F_{KUB2} that will provide the F_B approximation accuracy increasing in the attenuation zone compared to the F_{KUB}. In order to do this we create the system of equations

$$\begin{cases} A2\cdot cos(E)^3 + B2\cdot cos(E)^2 + C2\cdot cos(E) + D2 = 0.6, \\ A2\cdot cos(t)^3 + B2\cdot cos(t)^2 + C2\cdot cos(t) + D2 = Q, \\ A2\cdot cos(u)^3 + B2\cdot cos(u)^2 + C2\cdot cos(u) + D2 = G, \\ D2 = 0 \end{cases}$$

where $E = a\cos(e^{-0.511/n})$, 0.6 - the ordinate axis level of F_{KV} and F_{KUB2} connection

From the system we find that the coefficient $A2$ F_{KUB2} is calculated using the formula

$$0.2\frac{LR(3R-3L)+GR(5E^2-R5E)+LQ(L5E-5E^2)}{L^3(RE^2-R^2E)+L^2(R^3E-RE^3)-LR^2(RE^2-E^3)}.$$

The coefficient $B2$ is calculated using the fornula

$$0.2\frac{GR(R^2 5E-5E^3)+LR(3L^2-3R^2)+QL(5E^3-L^2 5E)}{L^3(RE^2-R^2E)+L^2(R^3E-RE^3)-LR^2(RE^2-E^3)}.$$

The coefficient $C2$ is calculated using the formula

$$0.2\frac{GR(R5E^3-R^2 5E^2)+L^2Q(L5E^2-5E^3)+LR(3LR^2-3L^2R)}{L^3(RE^2-R^2E)+L^2(R^3E-RE^3)-LR^2(RE^2-E^3)}.$$

The values of Q, G are set as $0.125, 1/32$.

Using the MS Excel tools the simplified polynomial formulas of these coefficients are obtained. The simplified formula of $A2$ is computed using the expression

$$(\frac{1}{2^4}+\frac{1}{2^6}+\frac{1}{2^{10}}+\frac{1}{2^{11}}+\frac{1}{2^{16}})n^2+(\frac{1}{2^3}+\frac{1}{2^4}+\frac{1}{2^7}+\frac{1}{2^8})n+(\frac{1}{2^7}+\frac{1}{2^8}-\frac{1}{2^{11}}).$$

The simplified formula of $B2$ is defined as

$$\begin{cases} -(\frac{1}{2^{16}}-\frac{1}{2^{20}})n^3-(\frac{1}{2^3}+\frac{1}{2^5}+\frac{1}{2^9}+\frac{1}{2^{14}})n^2+(\frac{1}{2^3}-\frac{1}{2^5}-\frac{1}{2^9})n+(\frac{1}{2^1}+\frac{3}{2^3}-\frac{1}{2^5}-\frac{1}{2^9})\, if\ n\ge 5 \wedge n<32 \\ -(\frac{1}{2^3}+\frac{1}{2^5}+\frac{1}{2^9}+\frac{1}{2^{10}}+\frac{1}{2^{16}})n^2+(\frac{1}{2^3}-\frac{1}{2^7}-\frac{1}{2^8}-\frac{1}{2^{10}}-\frac{1}{2^{11}})n+(\frac{1}{2^1}+\frac{1}{2^3}+\frac{1}{2^5}-\frac{1}{2^9})\, if\ n\ge 32 \wedge n\le 256 \end{cases}.$$

The simplified formula of $C2$ is computed using the formula

$$(\frac{1}{2^4}+\frac{1}{2^6}+\frac{1}{2^{10}}+\frac{1}{2^{11}})n^2-(\frac{1}{2^2}+\frac{1}{2^4}-\frac{1}{2^{10}}-\frac{1}{2^{11}})n+(\frac{1}{2^3}+\frac{1}{2^4}-\frac{1}{2^7}-\frac{1}{2^9}).$$

Fig. 2 shows the plots of F_{KUB2}, F_{KV}, F_B.

Therefore, the connection of F_{KUB2} and F_{KV} provides the highly accurate F_B approximation.

Let us find the F_{KUB2} and F_{KV} connection point. We solve the equation

$$0.786n\cdot\cos(\gamma)^2+(1-0.786n)\cdot\cos(\gamma)=A2\cdot\cos(\gamma)^3+B2\cdot\cos(\gamma)^2+C2\cdot\cos(\gamma).$$

The precise formula for the calculation of connection point $connect(n)$ between F_{KUB2} and F_{KV} when $n\ge 32$ is defined as

$$a\cos\left(\frac{1304125n^2-5360000+5522912n-\sqrt{15625n^4+8453383423744n^2-564728000n^3+31208448000000-16664864256000n}}{2(652125n^2+1632000n+92000)}\right).$$

The expression is calculated using the formula when $n < 32$

$$a\cos\left(\frac{-110336\cdot 10^3+1875n^3+20744\cdot 10^3 n^2+90990592n}{2(26112000n+10434000n^2+1472000)}-\right.$$
$$\left.-\frac{\sqrt{12808617984\cdot 10^6+86744733184\cdot 10^3 n^3+1636015759294464n^2-918864330752\cdot 10^4 n+3515625n^6+7779\cdot 10^7 n^5-473520128\cdot 10^4 n^4}}{2(26112000n+10434000n^2+1472000)}\right).$$

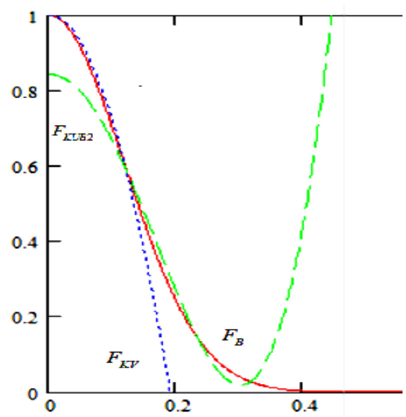

Figure 2. The plots of F_B, F_{KV}, F_{KUB2} .when $n = 70$

The simplified expression for $connect(n)$ is computed using the formula

$$\begin{cases}(\frac{1}{2^{12}}+\frac{1}{2^{18}})n^2-\frac{1}{2^6}n+(\frac{1}{2^1}-\frac{1}{2^4}-\frac{1}{2^6}-\frac{1}{2^7}-\frac{1}{2^9}) & if\ n<32\\ (\frac{1}{2^{16}}-\frac{1}{2^{20}}-\frac{1}{2^{21}})n^2-(\frac{1}{2^7}-\frac{1}{2^8}-\frac{1}{2^{10}}+\frac{1}{2^{15}})n+(\frac{1}{2^2}+\frac{1}{2^7}+\frac{1}{2^{10}}) & if\ n\ge 32 \wedge n<100\\ (\frac{1}{2^{20}})n^2-(\frac{1}{2^{11}}+\frac{1}{2^{14}}+\frac{1}{2^{15}})n+(\frac{1}{2^3}+\frac{1}{2^6}+\frac{1}{2^7}) & if\ n\ge 100\end{cases}.$$

At the ordinate axis level 0.6 the smooth connection of functions is provided because the difference of values between F_{KUB2} and F_{KV} near $connect(n)$ is insignificant (Fig. 3). Consequently, the derivatives calculation is not needed.

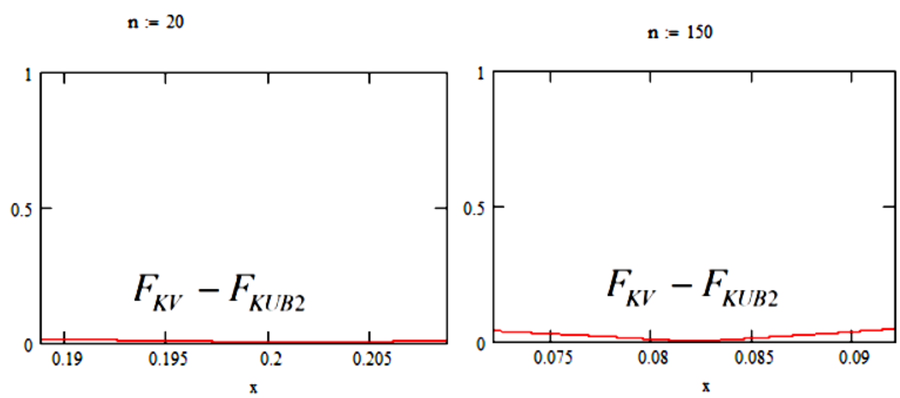

Figure 3. The deviations between F_{KV} and F_{KUB2} near $connect(n)$

Let us denote the developed combined function as F_{COMB}. Fig. 4 shows the plots of F_{COMB}, F_{KUB}, F_{KV}, F_B when $n = 36$.

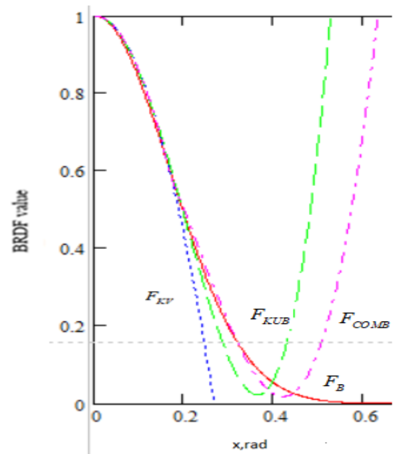

Fig. 4. The plots of F_{COMB}, F_{KUB}, F_{KV}, F_B when $n = 36$

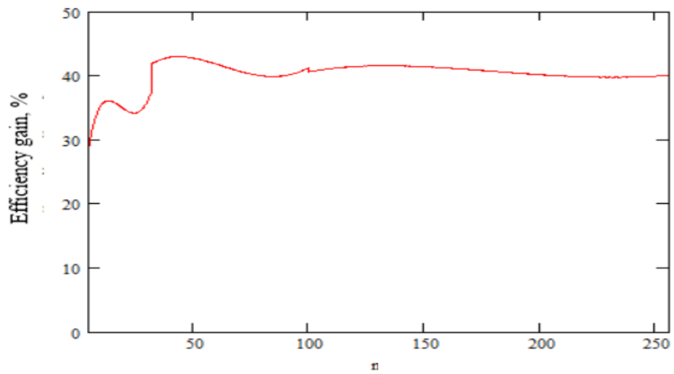

Figure 5. The plot of productivity gain from F_{COMB} calculation

Therefore, F_{COMB} provides the increasing of attenuation zone reproduction accuracy while speeding up the glare's epicenter zone calculations compared to F_{KUB}.

In average, the 40.2% of F_{COMB} curve length is calculated as F_{KV} (Fig. 5.), this value is a productivity gain.

Fig. 6 shows the plots of maximum relative errors δ between F_{COMB}, F_{KUB}, F_{KV} and F_B in the glare's epicenter for $n \in [5, 256]$.

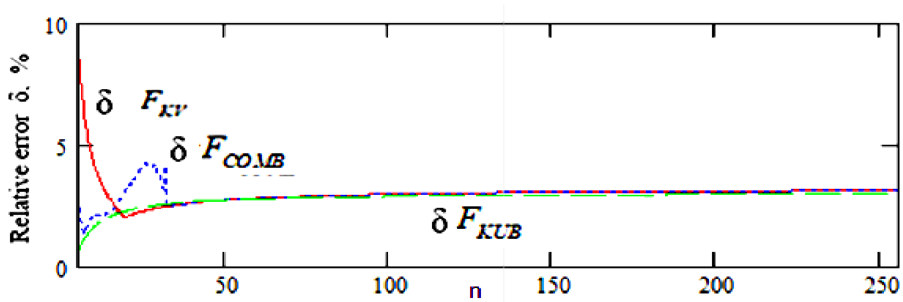

Figure 6. Plots of maximum relative errors between F_{COMB}, F_{KUB}, F_{KV} and F_B in the epicenter zone

Over the greater part of the interval $n \in [5, 256]$ the relative errors of the specified functions coincide and are equal to 3.04%.

Fig. 7. shows the plots of maximum absolute errors Δ between F_{COMB}, F_{KUB}, F_{KV} and F_B for $n \in [5, 256]$.

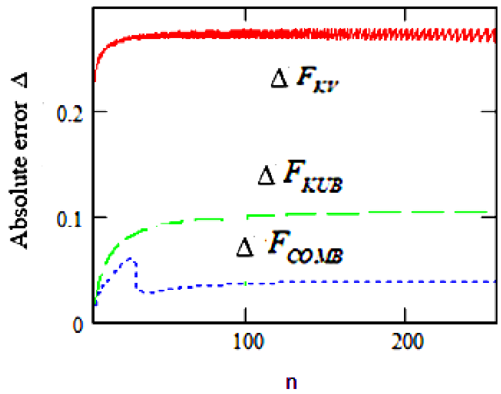

Fig. 7. The plots of maximum absolute errors between F_{COMB}, F_{KUB}, F_{KV} and F_B

The maximum Δ F_{KUB} is 0.1, maximum Δ F_{KV} – 0.28, maximum Δ F_{COMB} – 0.06.

Fig. 8 shows the results of applying F_{COMB}, F_{KUB}, F_{KV} to the visualization of the figures “Teapot”, “Robot” in BRDF Explorer.

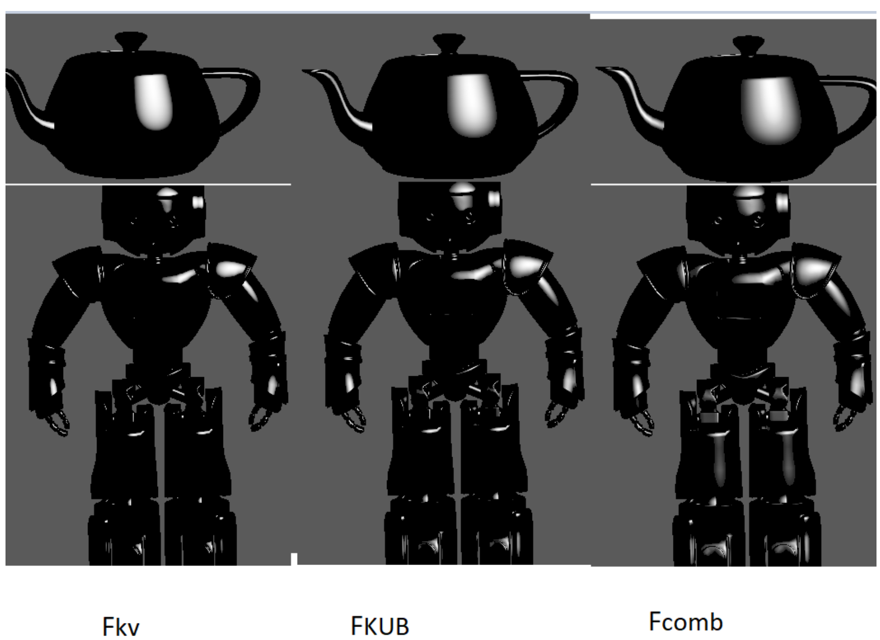

Fig. 8. The results of figures visualization based on F_{COMB}, F_{KUB}, F_{KV}

Therefore, F_{COMB} is characterized with the increased calculation productivity and more realistic glare’s attenuation zone reproduction.

4. CONCLUSIONS

In the article the combined reflectance model based on quadratic and modified cubic functions is proposed. The quadratic polynomial function corresponds to glare's epicenter zone, the cubic function corresponds to the attenuation zone.

The realism level of attenuation zone reproduction and the speed of model's coefficients calculations are improved through the modifying of cubic polynomial function. The productivity of BRDF calculation is increased by 40.2% through replacing the cubic function by quadratic in the epicenter zone.

Using the visualization of test figures in the software app BRDF Explorer it is shown that compared to quadratic and cubic models the proposed combined BRDF provides more accurate glares reproduction at the surfaces of objects.

REFERENCES

[1] Romanyuk, O., Romanyuk, O., Chekhmestruk, R., etc., "The Concept and Means of Adaptive Shading", in 2022 12th International Conference on Advanced Computer Information Technologies (ACIT), 33 – 38 (2022).

[2] Mikes, S. and Haindl, M., "Optimal Activation Function for Anistropic BRDF Modeling," in Proceedings of the 18th International Joint Conference on Computer Vision, Imaging and Computer Graphics Theory and Applications (VISIGRAPP 2023), 162 – 169 (2023).

[3] Romanyuk, O., "Classification of distribution functions of surface reflectivity," Scientific works of Donetsk National Technical University. Ser.: Informatics, cybernetics and computer technology, 9, 145 – 151 (2008).

[4] Khan, J., Malik, A., Kamel, N. and Dass, S., "Highlights removal using reflected energy and histogram analysis," Journal of Engg. Research, 7(1), 1 – 13 (2019).

[5] Romanyuk, O., Zavalniuk, Ye., Chekhmestruk, R., Mykhaylov, P. and Achanyar, H., "Combined bidirectional reflectance distribution functions usage for increasing images creation productivity," Applied Aspects of Information Technology, 6(2), 130 – 138 (2023).

[6] Löw, J., Kronander, J., Ynnerman A. and Unger, J., "BRDF Models for Accurate and Efficient Rendering of Glossy Surfaces," ACM Transactions on Graphics, 31(1), (2012).

[7] Montes, R. and Ureña, C., "An Overview of BRDF Models," University of Granada, Granada (2012).

[8] Kurt, M., "Real-Time Shading with Phong BRDF Model," DEU FMD, 21(63), 859 – 867 (2019).

[9] Miramirkhani, F. and Uysal, M., "Channel modelling for indoor visible light communications," Phil. Trans. R. Soc. A, 2169 (378), (2020).

[10] Bruckner, S., Grimm, S., Kanitsar, A. and Gröller, M., "Illustrative Context-Preserving Volume Rendering," in EUROGRAPHICS - IEEE VGTC Symposium on Visualization, (2005).

[11] Lytvynenko, V., Lurie, I., Voronenko, M., et al., "The use of Bayesian methods in the task of localizing the narcotic substances distribution," International Scientific and Technical Conference on Computer Sciences and Information Technologies, 2, 8929835, 60–63 (2019).

[12] Avrunin, O. G., Nosova, Y. V., Abdelhamid, I. Y., et al., 'Possibilities of automated diagnostics of odontogenic sinusitis according to the computer tomography data," Sensors (Switzerland), 21(4), 1-22 (2021).

[13] Avrunin, O.G.; Nosova, Y.V.; Abdelhamid, I.Y.; et al., "Research Active Posterior Rhinomanometry Tomography Method for Nasal Breathing Determining Violations," Sensors, 21, 8508 (2021).

[14] Pavlov, S.V., Kozhukhar, A.T., Titkov, S.V. et al., "Electro-optical system for the automated selection of dental implants according to their colour matching," Przeglad Elektrotechniczny, 93(3), 121–124 (2017).

[15] Wójcik, W., Pavlov, S., Kalimoldayev, M., "Information Technology in Medical Diagnostics II," London: Taylor & Francis Group, CRC Press, Balkema book, 336 (2019).

[16] Timchenko Leonid I. , Kokriatskaia Natalia I., et al., "Q-processors for real-time image processing,", Proc. SPIE 11581, Photonics Applications in Astronomy, Communications, Industry, and High Energy Physics Experiments 2020, 115810F (14 October 2020).